



RESEARCH LETTER

10.1002/2016GL072124

Key Points:

- There were three different transport pathways for spring Asian dust events in the study area
- Ocean primary productivity was significantly increased by the spring Asian dust events
- There has been a recent decrease in spring Asian dust events in the western North Pacific Ocean

Supporting Information:

- Supporting Information S1

Correspondence to:

I.-N. Kim,
ilnamkim@inu.ac.kr

Citation:

Yoon, J.-E., et al. (2017), Spatial and temporal variabilities of spring Asian dust events and their impacts on chlorophyll-*a* concentrations in the western North Pacific Ocean, *Geophys. Res. Lett.*, 44, 1474–1482, doi:10.1002/2016GL072124.

Received 8 DEC 2016

Accepted 1 FEB 2017

Accepted article online 2 FEB 2017

Published online 15 FEB 2017

Corrected 6 MAR 2017 and 9 MAY 2017

This article was corrected on 6 MAR 2017 and 9 MAY 2017. See the end of the full text for details.

Spatial and temporal variabilities of spring Asian dust events and their impacts on chlorophyll-*a* concentrations in the western North Pacific Ocean

Joo-Eun Yoon¹ , Kitae Kim² , Alison M. Macdonald³ , Ki-Tae Park² , Hyun-Cheol Kim²,
Kyu-Cheul Yoo² , Ho-Il Yoon², Eun Jin Yang², Jinyoung Jung² , Jae-Hyun Lim⁴ ,
Ju-Hyoung Kim⁵ , Jiyoung Lee¹ , Tae-Jun Choi¹ , Jae-Min Song¹, and Il-Nam Kim¹

¹Department of Marine Science, Incheon National University, Incheon, South Korea, ²Korea Polar Research Institute, Incheon, South Korea, ³Woods Hole Oceanographic Institution, Woods Hole, Massachusetts, USA, ⁴National Institute of Fisheries Science, Busan, South Korea, ⁵Faculty of Marine Applied Biosciences, Kunsan National University, Gunsan, South Korea

Abstract As the western North Pacific Ocean is located downwind of the source regions for spring Asian dust, it is an ideal location for determining the response of open waters to these events. Spatial analysis of spring Asian dust events from source regions to the western North Pacific, using long-term daily aerosol index data, revealed three different transport pathways supported by the westerly wind system: one passing across the northern East/Japan Sea (40°N–50°N), a second moving over the entire East/Japan Sea (35°N–55°N), and a third flowing predominantly over the Siberian continent (>50°N). Our results indicate that strong spring Asian dust events can increase ocean primary productivity by more than 70% (>2-fold increase in chlorophyll-*a* concentrations) compared to weak/nondust conditions. Therefore, attention should be paid to the recent downturn in the number of spring Asian dust events and to the response of primary production in the western North Pacific to this change.

1. Introduction

Over the last two and half decades, input of aeolian dust into the ocean environment has been regarded as an important research topic due to its potential effects on ocean primary productivity (OPP), carbon cycling, and climate change [Martin, 1990; Bopp et al., 2003; Jickells et al., 2005]. Global dust emission rate estimates range from ~1000 to 2200 Tg yr⁻¹ [Zender et al., 2004]. The most intense dust sources are the desert areas of the North Africa (i.e., Saharan dust) and the central Asia (i.e., Asian dust) [Mahowald et al., 2005]. Asian dust, originating in Taklimakan and Gobi Deserts, accounts for ~10–25% of global dust emission and is the second largest dust source globally [Tanaka and Chiba, 2006; Tegen and Schepanski, 2009].

As the western North Pacific Ocean (WNP) is located downwind from the source regions of Asian dust (Figure 1a), it is an ideal location for determining the response of open waters to these events. Supported by the westerly wind system, the supply of Asian dust to the WNP mainly occurs in spring (March–May) [Duce et al., 1980; Uematsu et al., 1983; Takemura et al., 2002]. The month of April, alone, is responsible for more than 50% of spring Asian dust events (Figure S1 in the supporting information) [Sun et al., 2001; Tan et al., 2012]. Modeling studies and short-term observations suggest that spring Asian dust is rapidly transported from its source regions across the WNP to North America by westerly winds [Duce et al., 1980; Uematsu et al., 1983; Husar et al., 2001; Logan et al., 2010]. However, the lack of large-scale and long-term observations means that little is known about the spatial and temporal variability of the transport pathways of spring Asian dust events.

Previous studies reported that concentrations of deposited iron observed during Asian dust events were much higher than those observed during the nondust periods, while the difference between dust and nondust events in deposited nitrate and total phosphorus concentrations was not nearly as dramatic [Kang et al., 2009; Kim et al., 2009; Furutani et al., 2010; Onishi et al., 2015]. Therefore, in the WNP ecosystem (colimited by iron and nitrogen [Moore et al., 2002; Liu et al., 2004; Krishnamurthy et al., 2009]), it is expected that, along the transport pathways of spring Asian dust, OPP is temporarily enhanced through relief of iron stress that acts as a limiting factor for the phytoplankton growth under nondust conditions [Duce and Tindale, 1991; Moore et al., 2002]. Recently, studies have reported a significant correlation between spring Asian dust events and

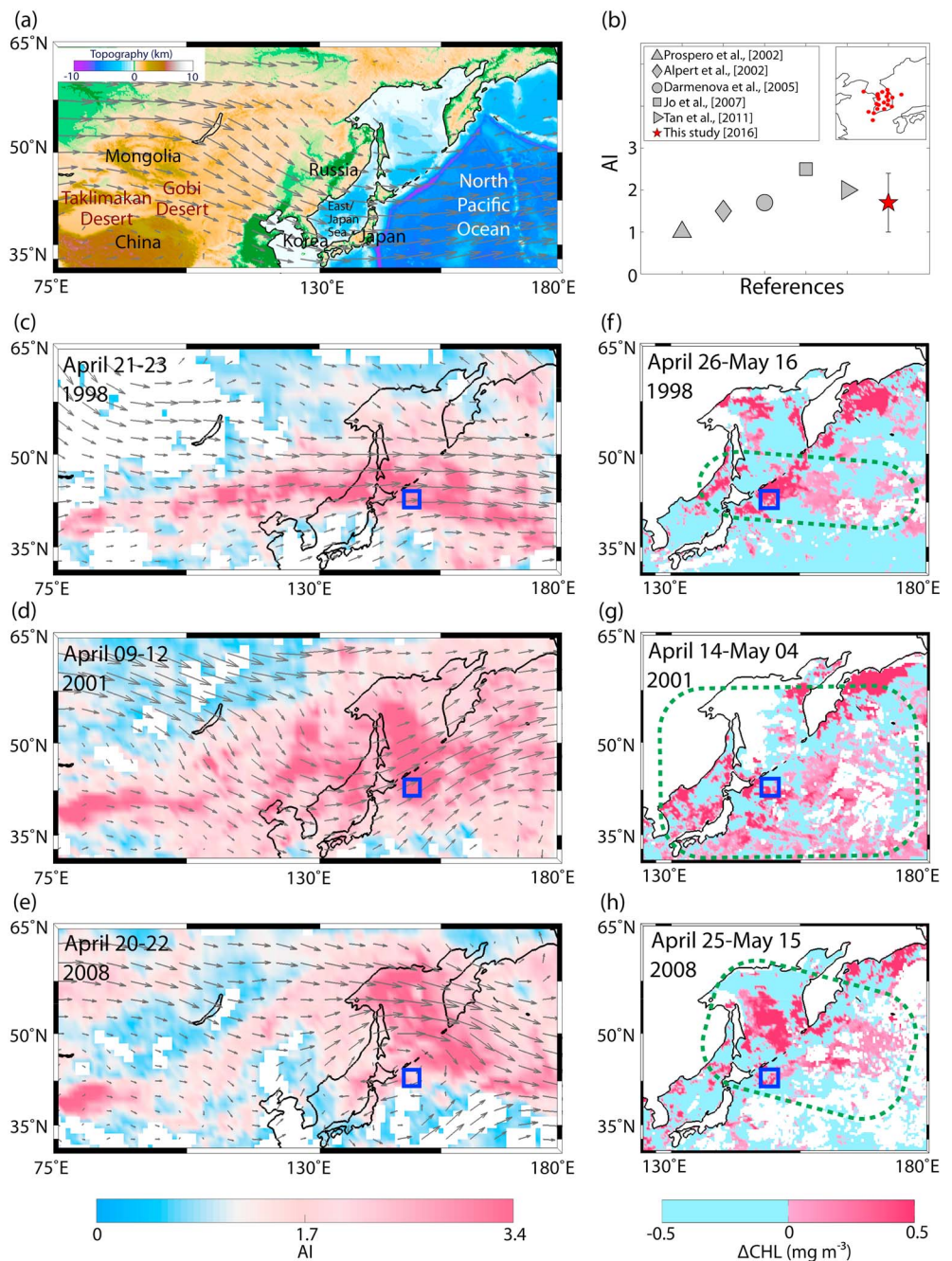


Figure 1. (a) Map illustrating the area of interest from central Asia to the western North Pacific Ocean (WNP) (30°N–65°N and 75°E–180°E). The color scale represents 2-Minute Gridded Global Relief Data (ETOPO2) topography (<http://rda.ucar.edu/datasets/ds759.3/>) [Bezdek and Sebera, 2013]. The grey arrows represent mean (1998–2014) spring winds at 700 hPa. (b) Published threshold aerosol index (AI) values used to determine the occurrence of dust events. The error bar used here (red star) indicates standard deviation from mean. The inset shows the location (red circles) of the 21 land-based KMA stations whose data were used in our analysis. Spatial distributions of AI for (c) 21–23 April 1998, (d) 9–12 April 2001, and (e) 20–22 April 2008, in the WNP, based on NASA’s Total Ozone Mapping Spectrometer (TOMS) (1998 and 2001) and Ozone Monitoring Instrument (OMI) (2008) satellite observations. The grey arrows represent mean National Centers for Environmental Prediction/National Center for Atmospheric Research (NCEP/NCAR) wind velocities at 700 hPa averaged over 5–6 days spanning dust events. Spatial distributions of ΔCHL (mg m^{-3}) for (f) 26 April to 16 May 1998, (g) 14 April to 4 May 2001, and (h) 25 April to 15 May 2008. The green dotted lines indicate the area in which the AI values exceeded the 1.7 threshold. The blue square (42°N – 44°N and 148°E – 150°E) indicates $2^{\circ} \times 2^{\circ}$ region in which AI exceeded the 1.7 threshold value more than three times, during each of the April timeframes. Data from this area were used for Figure 2.

OPP at the Kyodo North Pacific Ocean Time-series station in the WNP (44°N, 155°E) [Yuan and Zhang, 2006; Han et al., 2011]. WNP spring blooms are strongly influenced by surface mixed layer dynamics and availability of sunlight and occur over the same general season as the springtime dust events [Sverdrup, 1953; Yoshimori et al., 1995; Obata et al., 1996]. However, because the Asian dust events are episodic within the spring time-frame, until now, the relationship between these short-lived dust events and OPP has not been confirmed across the broader expanse of the WNP.

The purpose of this study is (1) to investigate the spatial and temporal variability of spring Asian dust events beginning at their source regions and extending into the WNP and (2) to determine their impacts on OPP in the WNP.

2. Methods

2.1. Data

The analysis of spring Asian dust event transport pathways presented here covers a 16 year period from 1998 to 2014 (note that the period of 2002–2004 was totally excluded from our analysis due to the lack of reliable observations; see Text S1 in the supporting information) and is based on a variety of parameters associated with satellite observations (e.g., aerosol index, wind velocity, chlorophyll-*a*, isolume depth, and precipitation) as well as the ocean temperature record from a reanalysis model. Aerosol index (AI) values that provide a measure of the magnitude of dust loading in the atmosphere [Herman et al., 1997; Torres et al., 2007] were used to investigate the transport pathways of spring Asian dust event. The 700 hPa (i.e., ~3 km above the Earth's surface) winds were used to represent the pathway for the active connection between dust sources in the atmosphere and the WNP [Husar et al., 2001; Satake et al., 2004]. Chlorophyll-*a* concentrations, indicating phytoplankton biomass [Steele, 1962; Cullen, 1982], were obtained for the study period from the Sea-viewing Wide Field-of-view Sensor (SeaWiFS) and Moderate Resolution Imaging Spectroradiometer (MODIS) Aqua satellites [O'Reilly et al., 2000; McClain, 2009]. Isolume depth, which defines the layer within which photosynthesis can occur in the upper water column, was estimated from the relationship between surface photosynthetically active radiation (PAR) and chlorophyll-*a* concentrations [Morel et al., 2007; Boss and Behrenfeld, 2010]. Isolume depth, corresponding to $\text{PAR} = 0.054 \text{ mol quanta m}^{-2} \text{ d}^{-1}$, was recently determined in the North Pacific Subtropical Gyre [Laws et al., 2014] and is typically expressed as $Z_{0.054}$. We use $Z_{0.054}$ to estimate the photosynthetic depth (i.e., isolume depth > mixed layer depth (MLD)) in our analysis. Precipitation (i.e., rain) was classified into four types based on magnitude [Liu, 2015]: (1) no rain, (2) light rain (<2.5 mm h⁻¹), (3) moderate rain (2.5–10 mm h⁻¹), and (4) heavy rain (>10 mm h⁻¹). MLD was estimated as the depth at which temperature is 0.2°C less than the temperature at 3 m (i.e., $T_{\text{at } 3 \text{ m}} - T_{\text{a depth}} = 0.2^\circ\text{C}$) [Thompson, 1976].

To investigate the impact of spring Asian dust events on OPP in the WNP, we used chlorophyll-*a*, isolume depth, precipitation, and MLD data. The OPP discussion in section 3.2 is based on OPP estimated from satellite-based chlorophyll-*a* concentrations by using an appropriate OPP algorithm, which was redeveloped by adding primary productivity data set measured by the ¹³C method in the WNP [Kameda and Ishizaka, 2005]. Further details are provided in Text S1.

2.2. Definition of Spring Asian Dust Events Based on Aerosol Index

Satellite-based AI estimates have been widely used as a key parameter in spatial and temporal analyses of dust events [Herman et al., 1997; Prospero et al., 2002]. AI estimates act as indicators to determine whether dust events occur in particular source regions and to trace the pathway along which they are transported. A threshold value is set, and AI values greater than the threshold are generally regarded as occurrence of dust events. Previous studies have suggested threshold values from 1.0 to 2.5 based on the spatial distribution of AI values in various particular dust source regions (see Figure 1b) [Alpert et al., 2002; Prospero et al., 2002; Darnenova et al., 2005; Jo et al., 2007; Tan et al., 2011]. To find an optimal AI threshold associated with the occurrence of spring Asian dust events in our study area, we used reports from the 21 land-based Korea Meteorological Administration (KMA) stations on the spring Asian dust that occurred between 1998 and 2014, as there are no ocean-based stations providing in situ observations on Asian dust to determine its onset and duration. In addition, the station locations are downwind of Asian dust source regions (Figure 1a), representing that the KMA stations are directly influenced by the Asian dust events due to geographic proximity to

the source regions, and the transport of Asian dust via westerly winds is quite fast, suggesting that the gradient in the AI values from the source regions to the 21 KMA stations is not large. We focused the analysis particularly on those reports dealing with severe dust events—PM₁₀ (particulate matter less than 10 μm in diameter) $> 400 \mu\text{g m}^{-3}$ for at least 2 h in a dust day (<http://www.kma.go.kr>). Based on these criteria, the AI values from 21 KMA land-based observation stations (see the inset in Figure 1b), suggesting the occurrence of severe dust events, were identified, sorted, and averaged. The mean AI value, to be employed as the threshold for recognition of dust events in our analysis, was estimated to be 1.7 with a standard deviation of 0.7 ($n = 98$). This threshold AI value is comparable with the published estimates for various other regions [Alpert *et al.*, 2002; Prospero *et al.*, 2002; Darnenova *et al.*, 2005; Jo *et al.*, 2007; Tan *et al.*, 2011] (Figure 1b). The AI values were classified into three types based on their magnitude: (1) nondust event (AI < 1.7), (2) weak dust event (AI 1.7–2.5), and (3) strong dust event (AI > 2.5). In the study area, about 8% of all AI values reported between 1998 and 2014 were identified as spring Asian dust events (i.e., AI > 1.7) (Figure S2), where the term “spring” is defined as March through May.

3. Results and Discussion

3.1. Spatial and Temporal Variability

To analyze the spatial distribution of the spring Asian dust events between 1998 and 2014, we mapped the number of dust event days (i.e., those with AI > 1.7) over an area from central Asia to the WNP (30°N, 75°E to 65°N, 180°E) (Figure S3). Overall, the dust event day totals were greatest (> 30 spring days) in the source regions (i.e., Gobi and Taklimakan Deserts) and lower over the WNP ($< \sim 10$ days). This pattern of eastward decrease in dust days from the source regions to the WNP is consistent with a simulation of dust deposition [Uematsu *et al.*, 2003].

By using the daily AI values with each $1^\circ \times 1^\circ$ pixel in the WNP (Figure S4a) for each spring day, it was determined that the individual Asian dust events were sporadic (i.e., episodic), showing no discernible pattern over the study period (Figures S4b–S4o). However, AI values greater than 1.7 were concentrated in the month of April (pixel number: $\sim 20,000$) (Figure S5a), which had nearly as many dust days as March (pixel number: $\sim 11,000$) and May (pixel number: $\sim 12,000$) combined. In addition, the distribution of April AI values greater than 1.7 was spread over a much larger geographical area than the March and May distributions (Figures S5b–S5d), suggesting that April is a crucial time for spring Asian dust event research not only because of the number events [Sun *et al.*, 2001; Lee *et al.*, 2006; Tan *et al.*, 2012] but also because of the broad geographical reach of April events. Only in 1998 (21–23 April, 5 May, and 16–17 May), 2000 (8–9 May), 2001 (9–12 April), and 2008 (20–22 April) did the mean AI value averaged over the entire study area exceed the 1.7 threshold (solid red lines in Figures S4b–S4o). These 2 to 3 day periods are interpreted as particularly strong and significant spring Asian dust events.

To determine specific transport pathways from the source regions to and across the WNP, we focused on the April 1998, 2001, and 2008 dust events as they were substantially stronger and had broader impact than the others (Figures S6 and S7). Based on the geographical AI distributions for these events, three different spatial patterns were discerned (Figures 1c–1e): the first passed across the northern East/Japan Sea (40°N–50°N; April 1998), the second covered the entire East/Japan Sea (35°N–55°N; April 2001), and the third flowed predominantly over the Siberian continent ($> 50^\circ\text{N}$; April 2008). Not surprisingly, these patterns appear to be correlated with variations of westerly wind direction (Figures 1c–1e). For example, strong westerly winds in April 1998 developed in a narrow band leading to an Asian dust event (AI > 1.7) that moved eastward, passing over the East/Japan Sea and the WNP, also along a narrow band (40°N–50°N; Figure 1c) [Husar *et al.*, 2001]. In April 2001, strong westerly winds developed over a somewhat broader band, which led to an Asian dust event that moved into the WNP affecting the entire East/Japan Sea (Figure 1d). A pattern similar to this observed event was described in a numerical experiment modeling the transport of this April 2001 Asian dust event [Zhao *et al.*, 2003]. The westerly winds in April 2008 blew predominantly over northeastern Asia before extending into the WNP through the Okhotsk Sea. The Asian dust event resulting from these winds was transported over Siberia from the source regions and then spread into the WNP (Figure 1e). In summary, the month of April appears to be the best time for determining transport pathways for the major spring Asian dust events, and wind patterns are key factor for determining the geographical spread of dust both over the continent and the WNP.

3.2. Impacts on Chlorophyll-*a* Concentrations

As a form of “natural iron fertilization” capable of increasing OPP, dust events have been frequently linked to climate change both on glacial-interglacial time scales and in modern times [Martin, 1990; Kohfeld and Harrison, 2001; Bopp *et al.*, 2003]. Bishop *et al.* [2002] reported that production of particulate organic carbon increased sharply 5 days after an Asian dust event reached the eastern North Pacific Ocean near Station Papa. It continued to increase for 2 weeks beyond the arrival of the dust event. Another study conducted in the East/Japan Sea (Figure 1a) linked spring bloom in this marginal sea with Asian dust events occurring between 1998 and 2002 [Jo *et al.*, 2007]. As the WNP region of study presented here is located directly downwind and lies in closer proximity to the source regions of Asian dust than Station Papa in the far eastern Pacific, it is reasonable to hypothesize that WNP OPP can also be correlated with the dust events. It is the link that we seek to confirm. As in iron-stressed systems the addition of iron may lead to an increase in chlorophyll-*a* concentrations only, without an associated increase in OPP [Behrenfeld *et al.*, 2009], here we assume that surface chlorophyll-*a* concentrations can be used to represent surface OPP and therefore to estimate changes in OPP due to dust events.

To investigate the response of OPP to spring Asian dust events in the WNP, we first examined the spatial distribution of chlorophyll-*a* anomalies within ~5–10 days after the onset of the 1998, 2001, and 2008 spring Asian dust events. Chlorophyll-*a* anomalies (ΔCHL) assumed to represent the chlorophyll-*a* response to dust events were defined as $\Delta\text{CHL}_{\langle\text{year}\rangle} = \text{CHL}_{\langle\text{year}\rangle} - \text{CHL}_{\text{mean}}$, where $\text{CHL}_{\langle\text{year}\rangle}$ is the concentration for a particular year (here 1998, 2001, or 2008) defined as the composite over a 3 week period beginning with a lag of 5 days after the onset of the Asian dust event (e.g., for the 21–23 April 1998 event, CHL_{1998} is the composite from 26 April to 16 May 1998); CHL_{mean} is the temporal average chlorophyll-*a* concentration calculated over the same period from all years (e.g., the 1998 CHL_{mean} is based on all 26 April to 16 May periods between 1998 and 2014). Specific dates are provided in the legends of Figures 1f–1h. The 5 day lag time was derived from previous studies that reported North Pacific OPP stimulated by dust within ~5–10 days of particular dust events [Young *et al.*, 1991; Bishop *et al.*, 2002; Shi *et al.*, 2012]. In spite of some obscuration due to cloud interference, the overall spatial distribution of positive ΔCHL in 1998, 2001, and 2008 was generally consistent with the distribution of AI values >1.7 (Figures 1c–1h), broadly implying a probable cause-and-effect relationship (Figure S8).

The second step in the investigation involved an intensive temporal analysis in a smaller area to elucidate this relationship (42°N–44°N and 148°E–150°E; blue square in Figures 1c–1h). This particular area was selected because here not only did the April AI values collectively exceed the threshold 1.7 in 1998, 2001, and 2008 but also there was greater availability of data as chlorophyll-*a* images were less influenced by cloud interference compared to other areas (Figures S9 and S10). In addition, it is known that there is a dearth of cloud cover compared to the south of the Kuroshio Extension where clouds form in the unstable atmosphere that lies above the warmer Kuroshio waters [Tomita *et al.*, 2013]. In this area, the temporal variability of springtime AI and chlorophyll-*a* was compared in strong dust and weak/nondust years (Figure 2). Examining the structure of MLD and $Z_{0.054}$ (see the insets in Figures 2a and 2c), representing the conditions (i.e., nutrient supply, stratification, and irradiance) that drive a typical spring bloom [Sverdrup, 1953; Obata *et al.*, 1996], we identified two distinguishable sets of springtime conditions: one in which the MLD shoals with time, e.g., 1998 (strong dust year) and 2010 (weak dust year [Tan *et al.*, 2016, 2017]), and a second in which the MLD fluctuates, e.g., 2001 (strong dust year) and 2014 (nondust year).

The water column structures of MLD and $Z_{0.054}$ were identical in the spring of 1998 and 2010 (see Figure 2a inset), indicating that the conditions for typical spring blooming were similar. However, it is evident that the chlorophyll-*a* pattern in these two years was different (Figures 2a and 2b). In the spring of 2010, a weak dust year, the concentrations of chlorophyll-*a* were quite constant with time and were relatively low ($<2 \text{ mg m}^{-3}$) compared to the mean values averaged for the 1998–2014 spring (Figure 2a). On the other hand, the concentrations of chlorophyll-*a* in the spring of 1998, a strong dust year, rapidly increased to $>2 \text{ mg m}^{-3}$ (mean chlorophyll-*a* $\sim 1.4 \text{ mg m}^{-3}$) with a lag time of ~ 10 days after a strong dust event (AI > 2.5) on approximately April 20 and then peaked at a maximum of 5.3 mg m^{-3} (Figure 2b). The increasing trend was maintained for ~ 15 days (see a shadow zone in Figure 2b).

Another pair of years, 2001 (strong dust year) versus 2014 (nondust year), illustrates a different MLD tendency (i.e., fluctuation with time; Figure 2c inset) as compared to shoaling with time just discussed for 1998 and 2010

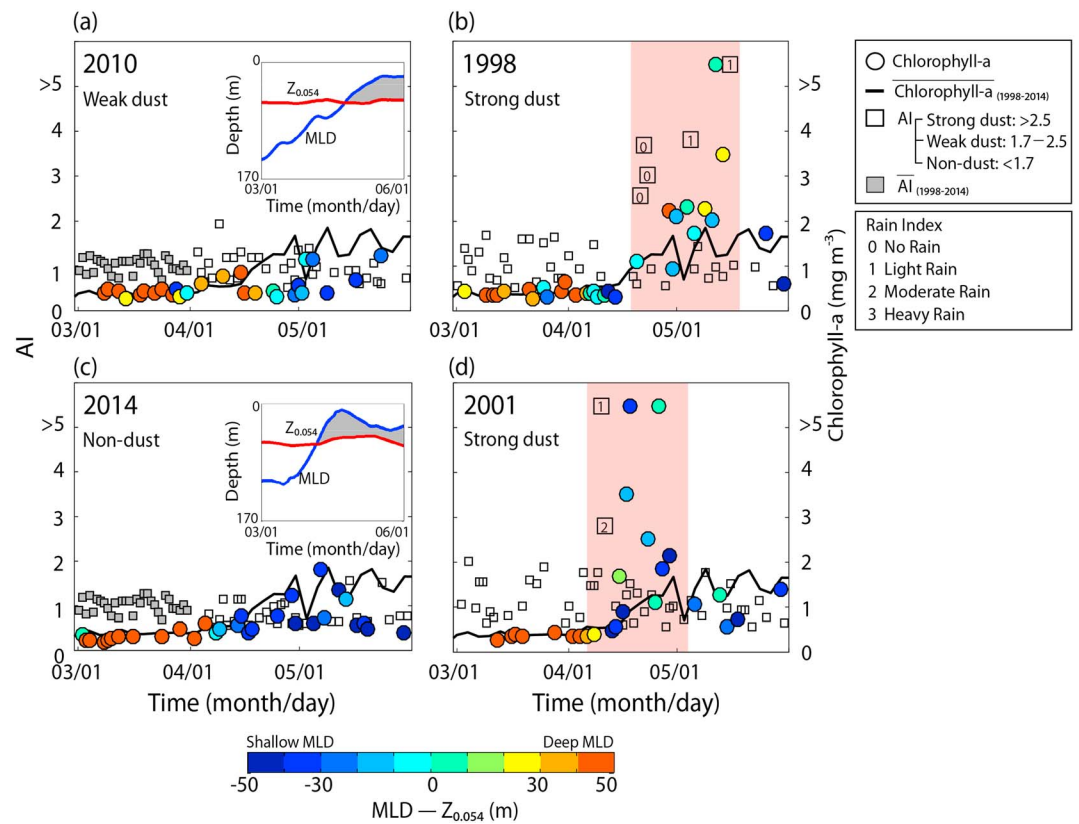


Figure 2. Daily AI values (black squares) and daily chlorophyll-*a* concentrations (mg m^{-3} , circles) during the spring of (a) 2010 (weak dust event), (b) 1998 (strong dust event), (c) 2014 (nondust event), and (d) 2001 (strong dust event) in the WNP (blue square in Figures 1c–1h). The filled black squares indicate AI values replaced with average 1998–2014 March values (Figures 2a and 2c). The black solid line indicates springtime trend in 1998–2014 mean chlorophyll-*a* concentrations (3 day composite). The pink shading highlights enhanced chlorophyll-*a* feature driven by strong spring Asian dust. The color scale represents difference between mixed layer depth (MLD) and isolume depth ($Z_{0.054}$): the negative values and grey zones in the insets indicate favorable conditions for active photosynthesis. The numbers in AI squares indicate the magnitude of precipitation during strong dust events.

(Figure 2a inset). As shown above, the spring of 2001 developed a shaped-peak of chlorophyll-*a* (maximum 6.3 mg m^{-3}) with a lag time of ~ 5 days after the strong dust event (AI > 2.5) on approximately April 10 (Figure 2d), whereas such a dramatic increase is not seen in the spring of 2014 (Figure 2c). The patterns of temporal interplay between MLD and $Z_{0.054}$ associated with the 2008 and 1998 dust events were similar. However, the earlier event has been chosen for illustration here because there were relatively more satellite-based chlorophyll-*a* data available (Figure S10). Nevertheless, although their increase was not quite as dramatic, the 2008 chlorophyll-*a* concentrations increased to $>2.0 \text{ mg m}^{-3}$ (i.e., compared to mean value 1.6 mg m^{-3}) after the strong dust event (Figure S11). We also identified a significant relationship between dust events and chlorophyll-*a* in the East/Japan Sea through a comparison of strong dust year (2006) versus nondust year (2014) (see Text S2 and Figure S12). The lag times (~ 5 – 10 days) were consistent with the results from the previous natural/artificial iron studies [Bishop *et al.*, 2002; Tsuda *et al.*, 2005].

Dust deposition can alter the water clarity and change the attenuation of light by increasing the concentration of suspended materials at ocean surfaces [Claustre *et al.*, 2002; Stramski *et al.*, 2004; Ohde, 2016], so Asian dust events may affect satellite-based chlorophyll-*a* concentrations. However, our results showed that the response of chlorophyll-*a* to strong Asian dust events was delayed with the lag times of 5–10 days (Figure 2). We are not sure if this delay (i.e., lag time) is due to the lack of light availability. A future study based on in situ observations is needed to accurately explain this delay phenomenon.

Dust deposition to the ocean occurs under both wet and dry conditions. In general, iron solubility through dry deposition is <0.8 – 2.1% in typical seawaters (pH ~ 8.0) [Jickells and Spokes, 2001]. However, iron is more soluble ($\sim 14\%$) under wet deposition (i.e., precipitation with pH ~ 4 – 7). For this reason, wet deposition has

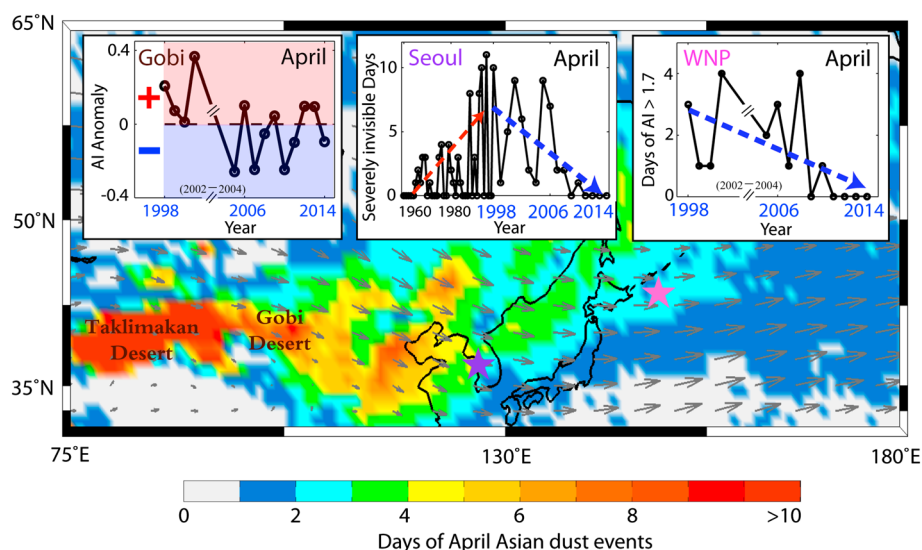


Figure 3. Recent decreasing trend of the spring Asian dust events. The first inset shows AI anomaly in the Gobi Desert during the month of April for the years of the study. AI anomalies were calculated as the difference between the individual April and the mean April values. The red plus and blue minus signs indicate AI anomaly >0 and AI anomaly <0 , respectively. The second inset shows April severely invisible days (traditional method used to define dust events), observed in Seoul station (purple star) of KMA during April 1960–2014 where linear regression analysis ($r^2 = 0.44$, P value < 0.05) suggests a decreasing trend for April 1998–2014. The third inset shows the days with AI > 1.7 in the WNP area 42°N – 44°N , 148°E – 150°E (pink star; same as the blue square in Figures 1c–1h) where linear regression analysis ($r^2 = 0.32$, P value < 0.05) again suggests decreasing trend for April 1998–2014. The color scale indicates the days of April Asian dust events (i.e., AI > 1.7) averaged during April 1998–2014 (except for 2002–2004). The grey arrows represent the mean wind vectors at 700 hPa during April 1998–2014.

been associated with an increased number of bioavailable iron forms [Sunda, 2001; Jickells and Spokes, 2001], which can be more effective at increasing chlorophyll-*a* concentrations [Gao *et al.*, 2003; Jo *et al.*, 2007]. During the strong spring Asian dust events in 1998 and 2001, little-to-no ($< 2.5 \text{ mm h}^{-1}$) precipitation occurred, except for a moderate rain (2.5 – 10 mm h^{-1}) in April 2001 (Figures 2b and 2d). Our results do not suggest any significant difference in OPP associated with wet dust events. However, there is a need for multiple in situ studies for confirmation, as satellite-based rain data do not provide the necessary detail.

Our analysis suggests that spring Asian dust events were episodic and chlorophyll-*a* concentrations in the WNP increased dramatically after dust events. Assuming that increases in chlorophyll-*a* concentrations are significantly correlated to the increases in phytoplankton biomass, we estimated OPP in the WNP (42°N – 44°N and 148°E – 150°E ; blue square in Figures 1c–1h) (see Text S1). It was found that OPP increased by more than 70% (> 2 -fold increase in chlorophyll-*a* concentrations) under strong dust event conditions (OPP_{1998} : $740 \pm 220 \text{ mg C m}^{-2} \text{ d}^{-1}$, OPP_{2001} : $670 \pm 210 \text{ mg C m}^{-2} \text{ d}^{-1}$) as compared to the weak/nondust conditions (OPP_{2010} : $430 \pm 100 \text{ mg C m}^{-2} \text{ d}^{-1}$, OPP_{2014} : $340 \pm 80 \text{ mg C m}^{-2} \text{ d}^{-1}$) (Table S1 in the supporting information). Recent studies report that occurrence of the spring Asian dusts declined in the source regions [Hara *et al.*, 2006; Zhu *et al.*, 2008] owing to disturbance of the westerly wind pattern due to climate change. Accordingly, April AI anomalies have decreased in the Gobi Desert, April severely invisible days observed at the KMA Seoul station have decreased since the late 1990s, and simultaneously, days in the WNP with April AI exceeding the 1.7 criterion have decreased over the 1998–2014 study period (see Figure 3). Meanwhile, a recent study reports that atmospheric nitrogen deposition has significantly increased in the North Pacific Ocean for the last three decades [Kim *et al.*, 2014], relieving nitrogen limitation. All this suggests that future study in the WNP investigating the effect on the OPP of the contrasting behavior of iron (i.e., decreasing trend) and nitrogen (i.e., increasing trend) inputs is needed.

4. Conclusions

We investigated the spatial and temporal dynamics of spring Asian dust events in the WNP and their impacts on OPP during the period of 1998–2014 (except for 2002–2004) in the WNP. We found three different transport pathways: one passing across the northern East/Japan Sea (40°N – 50°N), a second moving over the entire

East/Japan Sea (35°N–55°N), and a third moving predominantly over the Siberia continent (>50°N). The spatial patterns appear to be mainly determined by the westerly wind system. OPP (estimated from chlorophyll-*a* concentrations) increased by more than 70% (>2-fold increase in chlorophyll-*a* concentrations) following strong spring Asian dust events compared to weak/nondust times in the WNP. Although the dust events are episodic, their potential for sequestering atmospheric CO₂ via the “biological pump” may be considerable. The OPP response to the recent decreasing trend in spring Asian dust events is contrasted by its response to increasing atmospheric nitrogen deposition, as both inputs are required to revive this nitrogen/iron colimited ocean environment. It therefore behooves us to pay attention to possible future changes in OPP in the WNP.

Acknowledgments

This study was supported by the National Research Foundation of Korea (NRF) grant funded by the Korean government (MSIP) (2015R1C1A1A01052051). Funding for this work was partly provided by the Korea Polar Research Institute (KOPRI) project (PE17030). This research was a part of the project titled “Korean Iron Fertilization Experiment in the Southern Ocean (KOPRI, PM 16060)” funded by the Ministry of Oceans and Fisheries, Korea. A.M. Macdonald was supported by NOAA grant NA11OAR4310063 and internal WHOI funding. K.-T. Park was partly supported by KOPRI project PE17010. J.-H. Kim was partly supported by the program of “Management of Marine Organisms Causing Ecological Disturbance and Harmful Effects” funded by KIMST/MOF. Thanks to the anonymous reviewers for their insightful comments and suggestions that have contributed to improve this paper. The SeaWiFS and MODIS data distributed by the Ocean Biology Processing Group were downloaded freely on Ocean Color Web (<http://oceancolor.gsfc.nasa.gov>), and the AI data generated by TOMS and OMI science team were freely available at website (<https://earthdata.nasa.gov>). Temperature data were obtained from the HYCOM/NCODA (<http://hycom.org>). Precipitation data and wind velocity data were obtained from TRMM (<http://pmm.nasa.gov>) and NCEP/NCAR (<http://www.esrl.noaa.gov/psd>). PM₁₀ data in this study were obtained from KMA (<http://www.kma.go.kr>).

References

- Alpert, P., S. O. Krichak, M. Tsidulko, H. Shafir, and J. H. Joseph (2002), A dust prediction system with TOMS initialization, *Mon. Weather Rev.*, *130*(9), 2335–2345.
- Behrenfeld, M. J., et al. (2009), Satellite-detected fluorescence reveals global physiology of ocean phytoplankton, *Biogeosciences*, *6*(5), 779–794, doi:10.5194/bg-6-779-2009.
- Bezdek, A., and J. Sebera (2013), Matlab script for 3D visualizing geodata on a rotating globe, *Comput. Geosci.*, *56*, 127–130.
- Bishop, J. K. B., R. E. Davis, and J. T. Sherman (2002), Robotic observations of dust storm enhancement of carbon biomass in the North Pacific, *Science*, *298*(5594), 817–821.
- Bopp, L., K. E. Kohfeld, C. Le Quéré, and O. Aumont (2003), Dust impact on marine biota and atmospheric CO₂ during glacial periods, *Paleoceanography*, *18*(2), 1046, doi:10.1029/2002PA000810.
- Boss, E., and M. Behrenfeld (2010), In situ evaluation of the initiation of the North Atlantic phytoplankton bloom, *Geophys. Res. Lett.*, *37*, L18603, doi:10.1029/2010GL044174.
- Claustre, H., A. Morel, S. B. Hooker, M. Babin, D. Antoine, K. Oubelkheir, A. Bricaud, K. Leblanc, B. Quéguiner, and S. Maritorena (2002), Is desert dust making oligotrophic waters greener?, *Geophys. Res. Lett.*, *29*(10), 1469, doi:10.1029/2001GL014056.
- Cullen, J. J. (1982), The deep chlorophyll maximum: Comparing vertical profiles of chlorophyll *a*, *Can. J. Fish. Aquat. Sci.*, *39*(5), 791–803.
- Darmenova, K., I. N. Sokolik, and A. Darmenov (2005), Characterization of east Asian dust outbreaks in the spring of 2001 using ground-based and satellite data, *J. Geophys. Res.*, *110*(D2), D02204, doi:10.1029/2004JD004842.
- Duce, R. A., and N. W. Tindale (1991), Atmospheric transport of iron and its deposition in the ocean, *Limnol. Oceanogr.*, *36*(8), 1715–1726.
- Duce, R. A., C. K. Unni, B. J. Ray, J. M. Prospero, and J. T. Merrill (1980), Long-range atmospheric transport of soil dust from Asia to the tropical North Pacific: Temporal variability, *Science*, *209*(4464), 1522–1524.
- Furutani, H., A. Meguro, H. Iguchi, and M. Uematsu (2010), Geographical distribution and sources of phosphorus in atmospheric aerosol over the North Pacific Ocean, *Geophys. Res. Lett.*, *37*, L03805, doi:10.1029/2009GL041367.
- Gao, Y., S.-M. Fan, and J. L. Sarmiento (2003), Aeolian iron input to the ocean through precipitation scavenging: A modeling perspective and its implication for natural iron fertilization in the ocean, *J. Geophys. Res.*, *108*(D7), 4221, doi:10.1029/2002JD002420.
- Han, Y., T. Zhao, L. Song, X. Fang, Y. Yin, Z. Deng, S. Wang, and S. Fan (2011), A linkage between Asian dust, dissolved iron and marine export production in the deep ocean, *Atmos. Environ.*, *45*(25), 4291–4298.
- Hara, Y., I. Uno, and Z. Wang (2006), Long-term variation of Asian dust and related climate factors, *Atmos. Environ.*, *40*(35), 6730–6740.
- Herman, J. R., P. K. Bhartia, O. Torres, C. Hsu, C. Seftor, and E. Celarier (1997), Global distribution of UV-absorbing aerosols from Nimbus 7/TOMS data, *J. Geophys. Res.*, *102*(D14), 16,911–16,922, doi:10.1029/96JD03680.
- Husar, R. B., et al. (2001), Asian dust events of April 1998, *J. Geophys. Res.*, *106*(D16), 18,317–18,330, doi:10.1029/2000JD900788.
- Jickells, T. D., et al. (2005), Global iron connections between desert dust, ocean biogeochemistry, and climate, *Science*, *308*(5718), 67–71.
- Jickells, T. D., and L. J. Spokes (2001), Atmospheric iron inputs to the oceans, in *The Biogeochemistry of Iron in Seawater*, edited by D. R. Turner and K. A. Hunter, pp. 85–121, John Wiley, Chichester, U. K.
- Jo, C. O., J.-Y. Lee, K.-A. Park, Y. H. Kim, and K.-R. Kim (2007), Asian dust initiated early spring bloom in the northern East/Japan Sea, *Geophys. Res. Lett.*, *34*, L05602, doi:10.1029/2006GL027395.
- Kameda, T., and J. Ishizaka (2005), Size-fractionated primary production estimated by a two-phytoplankton community model applicable to ocean color remote sensing, *J. Oceanogr.*, *61*(4), 663–672.
- Kang, C. H., W. H. Kim, H. J. Ko, and S. B. Hong (2009), Asian dust effects on total suspended particulate (TSP) compositions at Gosan in Jeju Island, Korea, *Atmos. Res.*, *94*(2), 345–355.
- Kim, I.-N., K. Lee, N. Gruber, D. M. Karl, J. L. Bullister, S. Yang, and T.-W. Kim (2014), Increasing anthropogenic nitrogen in the North Pacific Ocean, *Science*, *346*(6213), 1102–1106.
- Kim, N. K., H. J. Park, and Y. P. Kim (2009), Chemical composition change in TSP due to dust storm at Gosan, Korea: Do the concentrations of anthropogenic species increase due to dust storm?, *Water Air Soil Pollut.*, *204*, 165–175.
- Kohfeld, K. E., and S. P. Harrison (2001), DIRTMAP: The geological record of dust, *Earth Sci. Rev.*, *54*(1–3), 81–114.
- Krishnamurthy, A., J. K. Moore, N. Mahowald, C. Luo, S. C. Doney, K. Lindsay, and C. S. Zender (2009), Impacts of increasing anthropogenic soluble iron and nitrogen deposition on ocean biogeochemistry, *Global Biogeochem. Cycles*, *23*, GB3016, doi:10.1029/2008GB003440.
- Laws, E. A., R. M. Letelier, and D. M. Karl (2014), Estimating the compensation irradiance in the ocean: The importance of accounting for non-photosynthetic uptake of inorganic carbon, *Deep Sea Res.*, *93*, 35–40.
- Lee, H. N., Y. Igarashi, M. Chiba, M. Aoyama, K. Hirose, and T. Tanaka (2006), Global model simulations of the transport of Asian and Sahara dust: Total deposition of dust mass in Japan, *Water Air Soil Pollut.*, *169*(1), 137–166.
- Liu, Z. (2015), Comparison of versions 6 and 7 3-hourly TRMM multi-satellite precipitation analysis (TMPA) research products, *Atmos. Res.*, *163*, 91–101.
- Liu, H., K. Suzuki, and H. Saito (2004), Community structure and dynamics of phytoplankton in the western subarctic Pacific Ocean: A synthesis, *J. Oceanogr.*, *60*, 119–137.
- Logan, T., B. Xi, X. Dong, R. Obrecht, Z. Li, and M. Cribb (2010), A study of Asian dust plumes using satellite, surface, and aircraft measurements during the INTEX-B field experiment, *J. Geophys. Res.*, *115*, D00K25, doi:10.1029/2010JD014134.

- Mahowald, N. M., A. R. Baker, G. Bergametti, N. Brooks, R. A. Duce, T. D. Jickells, N. Kubilay, J. M. Prospero, and I. Tegen (2005), Atmospheric global dust cycle and iron inputs to the ocean, *Global Biogeochem. Cycles*, *19*, GB4025, doi:10.1029/2004GB002402.
- Martin, J. H. (1990), Glacial-interglacial CO₂ change: The iron hypothesis, *Paleoceanography*, *5*(1), 1–13, doi:10.1029/PA0051001p00001.
- McClain, C. R. (2009), A decade of satellite ocean color observations, *Annu. Rev. Mar. Sci.*, *1*(1), 19–42.
- Moore, J. K., S. C. Doney, D. M. Glover, and I. Y. Fung (2002), Iron cycling and nutrient-limitation patterns in surface waters of the World Ocean, *Deep Sea Res.*, *49*, 463–507.
- Morel, A., Y. Huot, B. Gentili, P. J. Werdell, S. B. Hooker, and B. A. Franz (2007), Examining the consistency of products derived from various ocean color sensors in open ocean (case 1) waters in the perspective of a multi-sensor approach, *Remote Sens. Environ.*, *111*(1), 69–88.
- Obata, A., J. Ishizaka, and M. Endoh (1996), Global verification of critical depth theory for phytoplankton bloom with climatological in situ temperature and satellite ocean color data, *J. Geophys. Res.*, *101*(C9), 20,657–20,667, doi:10.1029/96JC01734.
- Ohde, T. (2016), Saharan dust effects in different trophic areas off Northwest Africa, *Arab. J. Geosci.*, *9*, 216.
- Onishi, K., S. Otani, A. Yoshida, H. Mu, and Y. Kurozawa (2015), Adverse health effects of Asian dust particles and heavy metals in Japan, *Asia Pac J. Public Health*, *27*(2), NP1719–26.
- O'Reilly, J. E., et al. (2000), Ocean color chlorophyll *a* algorithms for SeaWiFS, OC2 and OC4: Version 4. SeaWiFS postlaunch technical report series, in *NASA Tech. Memo. 2000–206892*, edited by S. B. Hooker and E. R. Firestone, pp. 8–22, NASA Goddard Space Flight Center, Greenbelt, Md.
- Prospero, J. M., P. Ginoux, O. Torres, S. E. Nicholson, and T. E. Gill (2002), Environmental characterization of global sources of atmospheric soil dust identified with the NIMBUS 7 Total Ozone Mapping Spectrometer (TOMS) absorbing aerosol product, *Rev. Geophys.*, *40*(1), 1002, doi:10.1029/2000RG000095.
- Satake, S., I. Uno, T. Takemura, G. Carmichael, and Y. Tang (2004), Characteristics of Asian aerosol transport simulated with a regional-scale chemical transport model during the ACE-Asia observation, *J. Geophys. Res.*, *109*, D19S22, doi:10.1029/2003JD003997.
- Shi, J.-H., H.-W. Gao, J. Zhang, S.-C. Tan, J.-L. Ren, C.-G. Liu, Y. Liu, and X. Yao (2012), Examination of causative link between a spring bloom and dry/wet deposition of Asian dust in the Yellow Sea, China, *J. Geophys. Res.*, *117*, D17304, doi:10.1029/2012JD017983.
- Sun, J., M. Zhang, and T. Liu (2001), Spatial and temporal characteristics of dust storms in China and its surrounding regions, 1960–1999: Relations to source area and climate, *J. Geophys. Res.*, *106*(D10), 10,325–10,333, doi:10.1029/2000JD900665.
- Sunda, W. G. (2001), Bioavailability and bioaccumulation of iron in seawater, in *The Biogeochemistry of Iron in Seawater*, edited by D. R. Turner and K. A. Hunter, pp. 41–84, Wiley, New York.
- Steele, J. H. (1962), Environmental control of photosynthesis in the sea, *Limnol. Oceanogr.*, *7*(2), 137–150.
- Stramski, D., S. B. Wozniak, and P. J. Flatau (2004), Optical properties of Asian mineral dust suspended in seawater, *Limnol. Oceanogr.*, *49*(3), 9–55.
- Sverdrup, H. U. (1953), On conditions for the vernal blooming of phytoplankton, *J. Cons. Perm.*, *18*(3), 287–295.
- Takemura, T., I. Uno, T. Nakajima, A. Higurashi, and I. Sano (2002), Modeling study of long-range transport of Asian dust and anthropogenic aerosols from East Asia, *Geophys. Res. Lett.*, *29*(24), 2158, doi:10.1029/2002GL016251.
- Tan, S.-C., G.-Y. Shi, J.-H. Shi, H.-W. Gao, and X. Yao (2011), Correlation of Asian dust with chlorophyll and primary productivity in the coastal seas of China during the period from 1998 to 2008, *J. Geophys. Res.*, *116*, G02029, doi:10.1029/2010JG001456.
- Tan, S.-C., G.-Y. Shi, and H. Wang (2012), Long-range transport of spring dust storms in Inner Mongolia and impact on the China seas, *Atmos. Environ.*, *46*, 299–308.
- Tan, S., J. Li, H. Gao, H. Wang, H. Che, and B. Chen (2016), Satellite-observed transport of dust to the East China Sea and the North Pacific Subtropical Gyre: Contribution of dust to the increase in chlorophyll during spring 2010, *Atmosphere*, *7*(11), 152, doi:10.3390/atmos7110152.
- Tan, S.-C., J. Li, H. Che, B. Chen, and H. Wang (2017), Transport of East Asian dust storms to the marginal seas of China and the southern North Pacific in spring 2010, *Atmos. Environ.*, *148*, 316–328.
- Tanaka, T. Y., and M. Chiba (2006), A numerical study of the contributions of dust source regions to the global dust budget, *Global Planet. Change*, *52*(1–4), 88–104.
- Tegen, I., and K. Schepanski (2009), The global distribution of mineral dust, *IOP Conf. Ser.: Earth Environ. Sci.*, *7*(1), 012001.
- Thompson, R. O. R. Y. (1976), Climatological numerical models of the surface mixed layer of the ocean, *J. Phys. Oceanogr.*, *6*(4), 496–503.
- Tomita, H., S.-P. Xie, H. Tokinaga, and Y. Kawai (2013), Cloud response to the meandering Kuroshio Extension Front, *J. Clim.*, *26*, 9393–9398, doi:10.1175/JCLI-D-13-00133.1.
- Torres, O., A. Tanskanen, B. Veihelmann, C. Ahn, R. Braak, P. K. Bhartia, P. Veefkind, and P. Levelt (2007), Aerosols and surface UV products from Ozone Monitoring Instrument observations: An overview, *J. Geophys. Res.*, *112*, D24547, doi:10.1029/2007JD008809.
- Tsuda, A., H. Kiyosawa, A. Kuwata, M. Mochizuki, N. Shiga, H. Saito, S. Chiba, K. Imai, J. Nishioka, and T. Ono (2005), Responses of diatoms to iron-enrichment (SEEDS) in the western subarctic Pacific, temporal and spatial comparisons, *Prog. Oceanogr.*, *64*(2–4), 189–205.
- Uematsu, M., R. A. Duce, J. M. Prospero, L. Chen, J. T. Merrill, and R. L. McDonald (1983), Transport of mineral aerosol from Asia over the North Pacific Ocean, *J. Geophys. Res.*, *88*(C9), 5343–5352, doi:10.1029/JC088iC09p05343.
- Uematsu, M., Z. Wang, and I. Uno (2003), Atmospheric input of mineral dust to the western North Pacific region based on direct measurements and a regional chemical transport model, *Geophys. Res. Lett.*, *30*(6), 1342, doi:10.1029/2002GL016645.
- Yoshimori, A., J. Ishizaka, T. Kono, H. Kasai, H. Saito, M. J. Kishi, and S. Taguchi (1995), Modeling of spring bloom in the western subarctic Pacific (off Japan) with observed vertical density structure, *J. Oceanogr.*, *51*(4), 471–488.
- Young, R. W., et al. (1991), Atmospheric iron inputs and primary productivity: Phytoplankton responses in the North Pacific, *Global Biogeochem. Cycles*, *5*(2), 119–134, doi:10.1029/91GB00927.
- Yuan, W., and J. Zhang (2006), High correlations between Asian dust events and biological productivity in the western North Pacific, *Geophys. Res. Lett.*, *33*, L07603, doi:10.1029/2005GL025174.
- Zender, C. S., R. L. L. Miller, and I. Tegen (2004), Quantifying mineral dust mass budgets: Terminology, constraints, and current estimates, *Eos Trans. AGU*, *85*(48), 509–512.
- Zhao, T. L., S. L. Gong, X. Y. Zhang, and I. G. McKendry (2003), Modeled size-segregated wet and dry deposition budgets of soil dust aerosol during ACE-Asia 2001: Implications for trans-Pacific transport, *J. Geophys. Res.*, *108*(D23), 8665, doi:10.1029/2002JD003363.
- Zhu, C., B. Wang, and W. Qian (2008), Why do dust storms decrease in northern China concurrently with the recent global warming?, *Geophys. Res. Lett.*, *35*, L18702, doi:10.1029/2008GL034886.

Erratum

In the originally published version of this article, Figures 1c-1e were marked with longitude “75°E to 180°E”, but the images represented “80°E to 180°E”. The images have been corrected to represent longitude “75°E to 180°E” as they are labeled.

In the original Acknowledgments, the KOPRI project funding number was incorrectly labeled as PP10610 and has been corrected to PE17030.

In the originally published version of the supporting information, we mistakenly used the Western North Pacific-estimated $Z_{0.054}$ (blue square shown in Figure 1; Lat: 42°N–44°N and Long: 148°E–150°E) instead of the East/Japan Sea-estimated $Z_{0.054}$ (red star; Lat: 43°N–45°N and Long: 138°E–140°E) for the calculation of ‘MLD – $Z_{0.054}$ ’ in Figure S12. However, this mistake does not affect our conclusions. We recalculated ‘MLD – $Z_{0.054}$ ’ with the East/Japan Sea-estimated $Z_{0.054}$, and then reproduced corrected Figure S12.

In Figure S12, color information indicates the magnitude of ‘MLD – $Z_{0.054}$ ’. Here, $Z_{0.054}$ is estimated as follows [Laws *et al.*, 2014]:

$$Z_{0.054} = \log\left(\frac{0.054}{0.98 \times \text{PAR}}\right) \left(\frac{Z_{\text{eu}}}{\log(0.01)}\right), \quad (\text{Supporting Information S2})$$

where PAR is surface photosynthetically available radiation ($\text{mol quanta m}^{-2} \text{d}^{-1}$), Z_{eu} is the euphotic zone depth where the photon flux reaches to 1% of the surface photon flux (m) [Ryther, 1956], and is calculated as [Morel *et al.*, 2007]:

$$\log_{10} Z_{\text{eu}} = 1.524 - 0.436 \times \text{CHL} - 0.0145 \times \text{CHL}^2 + 0.0186 \times \text{CHL}^3, \quad (\text{Supporting Information S3})$$

where CHL represents surface chlorophyll-a concentrations (mg m^{-3}).

These errors have been corrected, and the present version may be considered the authoritative version of record.